Available online at www.sciencedirect.com
ScienceDirect
Biochimica et Biophysica Acta 1758 (2006) 1018–1024
BIOCHIMICA ET BIOPHYSICA ACTA
BBA
www.elsevier.com/locate/bbamem

Water permeability of rat liver mitochondria: A biophysical study

Giuseppe Calamita [a,*], Patrizia Gena [a], Daniela Meleleo [b], Domenico Ferri [c], Maria Svelto [a]

[a] *Dipartimento di Fisiologia Generale ed Ambientale and Centro di Eccellenza di Genomica in campo Biomedico ed Agrario (CEGBA), Università degli Studi di Bari, Via Amendola 165/A, 70126 Bari, Italy*
[b] *Dipartimento Farmaco-Biologico, Università degli Studi di Bari, 70126 Bari, Italy*
[c] *Dipartimento di Zoologia, Laboratorio di Istologia e di Anatomia Comparata, Università degli Studi di Bari, 70126 Bari, Italy*

Received 29 October 2005; received in revised form 10 July 2006; accepted 14 July 2006
Available online 21 July 2006

Abstract

The movement of water accompanying solutes between the cytoplasm and the mitochondrial spaces is central for mitochondrial volume homeostasis, an important function for mitochondrial activities and for preventing the deleterious effects of excess matrix swelling or contraction. While the discovery of aquaporin water channels in the inner mitochondrial membrane provided valuable insights into the basis of mitochondrial plasticity, questions regarding the identity of mitochondrial water permeability and its regulatory mechanism remain open. Here, we use a stopped flow light scattering approach to define the water permeability and Arrhenius activation energy of the rat liver whole intact mitochondrion and its membrane subcompartments. The water permeabilities of whole brain and testis mitochondria as well as liposome models of the lipid bilayer composing the liver inner mitochondrial membrane are also characterized. Besides finding remarkably high water permeabilities for both mitochondria and their membrane subcompartments, the existence of additional pathways of water movement other than aquaporins are suggested.

Keywords: Volume homeostasis; Mitochondria; Outer membrane; Inner membrane; Water transport; Aquaporin

1. Introduction

Mitochondrial volume homeostasis is a housekeeping function, thought both to help regulate oxidative capacity [1], apoptosis [2,3], and mechanical signalling and to maintain the structural integrity of the organelle [4]. Mitochondrial volume changes are modulated by the net movement of solutes including K^+ and Ca^{2+} ions across the inner mitochondrial membrane (IMM) [4–6]. Although a number of mitochondrial transport systems have been identified and characterized for their ability to transport solutes across the mitochondrial membranes [7,8], the biophysics, and molecular mechanism and pathways for the movement of water remained completely elusive until the recent identification of an aquaporin water channel, AQP8, in the IMM of liver and many other tissues [9–11]. AQP8 immunostaining was found to be variable among mitochondria with heavy mitochondria being the more reactive ones. Another aquaporin, AQP9, was then found in the IMM of rat astrocytes and dopaminergic neurons [12]. Inhibition studies with the Hg^{++} ion, a known aquaporin blocker [13], indicated that AQP8 was not the only facilitated pathway for water moving through the liver inner membrane and that Hg^{++}-insensitive pathways other than aquaporins could exist in the IMM. Recently, no functional significant aquaporin expression was reported in rat and mouse liver mitochondria by Yang and coworkers [14]. The same Authors concluded that the observed millisecond osmotic equilibration was due to the high surface-to-volume ratio characterizing mitochondria (simple diffusion) rather than a high intrinsic membrane water permeability (facilitated transport). However, no experiments were addressed to evaluate the postulated water conductance of the voltage dependent anion channel (VDAC) and the permeability transition pore (PTP), two extraordinarily large pores of the mitochondrial membranes [2,7,15]. Further work is therefore needed to assess precisely the molecular pathways, biophysical properties and regulation of mitochondrial water transport.

Abbreviations: ANT, adenine nucleotide translocator; AQP, aquaporin; IMM, inner mitochondrial membrane; OMM, outer mitochondrial membrane; PBS, phosphate-buffered saline; PTP, permeability transition pore; VDAC, voltage-dependent anion channel

* Corresponding author. Tel.: +39 0805442928 (Office), tel.: +39 0805442453 (Laboratory); fax: +39 0805443388.
E-mail address: calamita@biologia.uniba.it (G. Calamita).

0005-2736/$ - see front matter © 2006 Elsevier B.V. All rights reserved.
doi:10.1016/j.bbamem.2006.07.008

In this study, while confirming the high water conductance of the IMM, we define the water permeability of rat liver mitochondria and related subcompartments such as the mitoplast and the outer membrane. The osmotic permeability of brain and testis mitochondria as well as that of liposome models of the IMM lipid bilayer were also defined.

2. Materials and methods

2.1. Isolation of mitochondria and preparation of mitoplasts and IMM and OMM vesicles

Mitochondria were prepared from adult male Wistar rats weighing 250–300 g (Morini, San Polo D'Enza, Italy). Rats were fed with a standard diet and water *ad libitum*. For all experiments, rats were decapitated after anesthesia and their livers, brains or testes were quickly removed and processed depending on the specific preparation. For the isolation of mitochondria, organs were homogenized with a Potter–Elvehjem homogenizer (4 strokes in 1 min at 500 rpm) in an *isolation medium* consisting of 220 mM mannitol, 70 mM sucrose, 20 mM Tris–HCl, 1 mM EDTA and 5 mM EGTA, pH 7.4. The homogenate was centrifuged at 500×*g* for 10 min at 4 °C and the pellet consisting of nuclei and unbroken cells was discarded; the resulting supernatant was centrifuged at 6000×*g* for 10 min at 4 °C and the related pellet was washed twice before being resuspended in *isolation medium* to which a cocktail of protease inhibitors had been added (1 mM PMSF, 1 mM leupeptin, 1 mM pepstatin A). Mitoplasts and vesicles of the outer and inner mitochondrial membrane were prepared as previously described [10]. The protein concentration was assayed by the Lowry method. All chemicals used for the preparations except digitonin (Calbiochem, La Jolla, CA) were from the Sigma Chemical Company (St. Louis, MO).

2.2. Immunoblotting analysis

Aliquots (60 μg of proteins) of isolated mitochondria, mitoplasts, or OMM and IMM vesicles prepared as above were heated to 90 °C and electrophoresed in an SDS/13% acrylamide gel (Mighty Small II, Amersham Biosciences, CA) using a low molecular weight protein ladder (Amersham Biosciences, Buckinghamshire, UK). The resolved proteins were transferred electrophoretically onto nylon membranes that were blocked in 5% (w/v) low fat milk in *blocking buffer* (20 mM Tris–HCl, 0.15 M NaCl, 1% Triton X-100, pH 7.5) for 1 h, and further incubated with affinity purified rabbit antibodies against VDAC (Abcam, Cambridge, UK), anti-prohibitin antibodies (Abcam, Cambridge, UK) or an immune serum directed to two peptides (QHASKQIAADKQYK and YDTAKGMLPDPKNVH) being conserved in all three isoforms of the adenine nucleotide translocator (ANT) kindly provided by Dr. Catherine Brenner at a final concentration of 2 and 1 μg/mL blocking solution, and a dilution of 1:1000 with blocking solution, respectively. Horseradish peroxidase antirabbit IgG treated membranes (anti-rabbit IgG peroxidase antibody, Sigma) were developed by luminal-chemiluminescence (ECL-Plus, Amersham Biosciences, Buckinghamshire, UK).

2.3. Electron microscopy

Pellets of the whole liver intact mitochondria, mitoplasts, outer and inner mitochondrial membrane vesicles, respectively, were fixed in a mixture of 3% paraformaldehyde and 1% glutaraldehyde in 0.1 mol/l PBS at pH 7.4 for 4 h at 4 °C. Specimens were postfixed in 1% OsO_4 in PBS for 60 min at 4 °C. Fixed specimens were dehydrated in ethanol and then embedded in Epon (TAAB, Reading, England). Ultrathin sections were mounted on Cu/Rh mesh grids. Finally, the sections were stained with uranyl acetate and lead citrate and observed using a Zeiss EM 109 electron microscope (Zeiss, Oberkochen, Germany).

2.4. Liposome technology

Liposomes with simple lipid bilayer membranes were prepared at 23 ± 1 °C by bath-sonicating a lipid solution composed of cardiolipin:phosphatidylethanolamine:phosphatidylcholine:phosphatidylinositol:sphingomyelin:cholesterol (18.5%:34.0%:39.5%:4.5%:2.0%:1.5%, respectively), corresponding to that of the rat liver inner mitochondrial membrane [16]. The lipid mixture was vortex mixed and incubated for 20 min at 0 °C. Liposomes were then formed at room temperature by rapidly injecting the mixture through a 23-gauge needle into 25 ml of the buffer used for preparing the mitochondria (*isolation buffer*) with a cocktail of protease inhibitors added to it.

2.5. Stopped flow light scattering

The size of the mitochondria, OMM and IMM vesicles, and artificial liposomes employed for the stopped-flow measurements was determined both with an N5 Submicron Particle Size Analyzer (Beckman Coulter Inc., Palo Alto, CA) and by morphometric analysis of electron micrographs. The time course mitochondrial, mitoplast, vesicular or liposome volume change was followed from changes in intensity of scattered light at the wavelength of 450 nm using a Jasco FP-6200 (Jasco, Tokyo, Japan) stopped-flow reaction analyzer which has a 1.6 ms dead time and 99% mixing efficiency in <1 ms. The sample temperature (20 °C in all experiments except the ones carried out to calculate of the Arrhenius activation energy) was controlled by a circulating water bath. Light scattering experiments were performed as previously described [10]. Briefly, 35 μl of a concentrated vesicle (or liposome) suspension was diluted into 2.5 ml of a hypotonic (220 mosM) *isolation medium* (124 mM mannitol, 70 mM sucrose, 20 mM Tris–HCl, 1 mM EDTA and 5 mM EGTA, pH 7.4). One of the syringes of the stopped-flow apparatus was filled with the specimen suspension, whereas the other was filled with the same buffer to which mannitol (or, in some experiments, sucrose) was added to reach a final osmolarity of 500 mosM in order to establish a hypertonic gradient (140 mosM) upon mixing. The final protein concentration after mixing was 100 μg/ml. Immediately after applying a hypertonic gradient, water outflow occurs, and the vesicles shrink, causing an increase in scattered light intensity. The data were fitted to a single exponential function and the related rate constant (K_i, s^{-1}) of the water efflux out of the analyzed specimen was measured. The osmotic water permeability coefficient (P_f), an index reflecting the osmotic water permeability of the vesicular membrane, was deduced from the K_i as described [17], using the equation:

$$P_f = K_i \cdot V_0 / A_v \cdot V_w \cdot \Delta C$$

where K_i is the fitted exponential rate constant, V_0 is the initial mean vesicle volume, A_v is the mean vesicle surface, V_w is the molar volume of water, and ΔC is the osmotic gradient. The medium osmolarity was verified by freezing point depression, using a Halbmikro-Osmometer (Knauer, Berlin, Germany). In some experiments, the samples were incubated for 5 min in *isolation medium* deprived of EGTA and EDTA and containing 300 μM $HgCl_2$, a sulfhydryl compound known to block mammalian aquaporins, including AQP8 [13]. In other experiments, to verify the blocking action of the Hg^{++} ion, the $HgCl_2$ treatment of the samples was followed by a 15 min exposure to 10 mM of the reducing agent β-mercaptoethanol. In order to evaluate whether the size of the experimental specimens was altered as a consequence of the Hg^{++} treatment, samples of each specimen were analyzed by quasi-elastic light scattering (N5 Submicron Particle Size Analyzer). The osmotic water permeability coefficient (P_f) was calculated as described in our previous work [10]. The temperature dependence of osmotic water permeability in the liver mitochondria was assessed by determining the Arrhenius activation energy (E_a) calculated by measuring the K_i of the mitochondria at 5, 15, 25 and 37 °C.

3. Results

3.1. Mitochondria, mitoplasts, liposomes and vesicles of the outer and inner mitochondrial membranes

Mitochondria were isolated from rat liver by a gravitational approach (6000 × g fraction) and then used to prepare mitoplasts, and OMM and IMM vesicles as well (see Materials and methods for details). The quality of the preparations was evaluated by immunoblotting and electron microscopy. The immunoreactive bands detected by using polyclonal antibodies

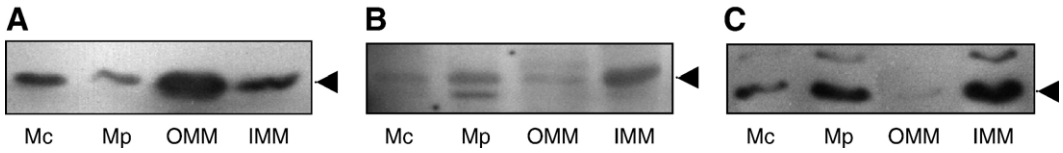

Fig. 1. Immunoblotting analysis of the rat liver mitochondria, mitoplast and OMM and IMM vesicle preparations used for the biophysical studies. (A) Immunoblotting using affinity-purified anti-VDAC antibodies. The VDAC immunoreactivity (31 kDa band; arrowhead) is strongly enriched in the outer membrane fraction. (B) Immunoblotting using an anti-ANT immune serum. The strong immunoreactivity is seen in the inner membrane fraction (32 kDa band; arrowhead). (C) Immunoblotting with affinity-purified anti-prohibitin antibodies. Remarkable prohibitin reactivity (30 kDa band; arrow) is detected in the IMM and mitoplast fractions. *Mc*, mitochondria; *Mp*, mitoplasts; *IMM*, inner mitochondrial membrane; *OMM*, outer mitochondrial membrane.

directed against marker proteins of the outer membrane, the voltage dependent anionic channel (VDAC) and the inner membrane, the adenine nucleotide translocator (ANT) and prohibitin are shown in Fig. 1A–C. As proof of the quality of the preparations the VDAC, ANT and prohibitin immunoreactivities were enriched in the OMM and IMM subcompartments, respectively (Fig. 1A–C and Table 1). Consistent with the above immunoblotting pattern as well as with our previous studies [10] high enrichment of mitochondria, mitoplasts, and OMM and IMM vesicles was observed in the gravitational pellets analyzed by electron microscopy (Fig. 2A, B). The mean diameters of the OMM and IMM vesicles as well as the ones of the IMM artificial liposomes used for the stopped-flow light scattering experiments (see below) were measured both by a particle size analyzer and morphometric analysis of electron micrographs (0.191±0.08, 0.281±0.08 and 0.193±0.029 μm, respectively).

3.2. Stopped flow light scattering analysis

Stopped flow light scattering was performed to characterize the overall water permeability of mitochondria, mitoplasts and the OMM and IMM vesicles. Liposomes were prepared as an experimental model to assess the extent of the IMM's diffusional water permeability.

Liver mitochondria, mitoplasts or vesicles were subjected rapidly to a hypertonic osmotic gradient (140 mosM) created by mannitol, and the time course of the related shrinkages was followed from the increase in scattered light. The data were fitted to measure the rate constant (K_i, s^{-1}) of the water efflux out of the analyzed specimen. In line with our previous study [10], as well as with the rapid changes of volume which the liver mitochondrial matrix is known to undergo [18] the rate constant of both mitochondria and mitoplasts was high: 22.98±3.7 and 23.74±3.3 s^{-1}, respectively (Fig. 3A, B; black histograms). The rate constants of whole intact mitochondria (6000×g fraction) isolated from brain and testis, two organs where AQP8 has been reported to be abundant and absent, respectively, were assessed in order to evaluate potential direct correlation between the high water permeability of mitochondria and the presence of the AQP8 water channel in the IMM [13,19,20]. Suggesting no major functional implication for AQP8 in overall mitochondrial water permeability, the K_i values of brain and testis mitochondria resulted high and of similar extent compared to the liver counterparts (Fig. 4). No significant differences were found between the diameters of the isolated brain, testis and liver mitochondria (data not shown).

Stopped flow light scattering was also carried out in order to dissect the water permeability of the liver mitochondrion at the

Table 1
Densitometric analysis of the relative enrichment of VDAC, ANT and prohibitin in submitochondrial fraction preparations

Submitochondrial marker	Submitochondrial fraction			
	Mc [a]	Mp	OMM	IMM
VDAC	100%	34±9%	726±45%	67±9%
ANT	100%	220±29%	23±8%	423±32%
Prohibitin	100%	346±19%	18±6%	889±49%

[a] The intensity of the immunoblotting band detected in the preparation of whole intact mitochondria (*Mc*) was arbitrarily taken as 100%. *Mp*, mitoplasts; *OMM*, outer mitochondrial membrane; *IMM*, inner mitochondrial membrane.

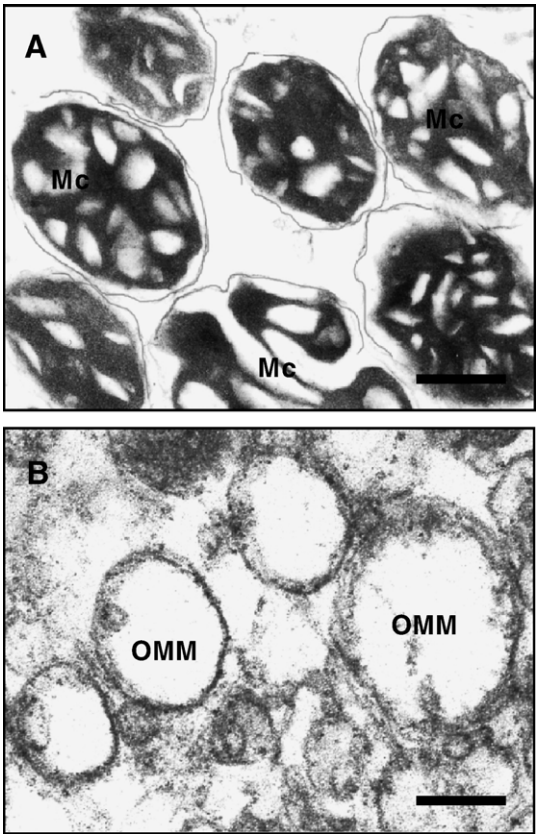

Fig. 2. Electron microscopy analysis. Electron micrographs showing samples of the mitochondria (A; *Mc*) and outer mitochondrial membranes (B; *OMM*) used for the light scattering study. Bars: A, 0.5 μm; B, 0.2 μm.

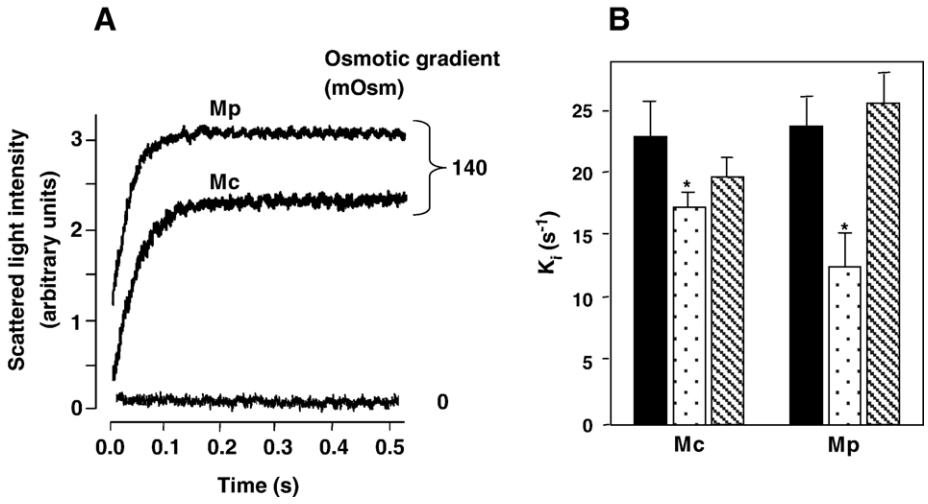

Fig. 3. Stopped flow light scattering of rat liver whole intact mitochondria and mitoplasts. (A) representative experiments of stopped flow light scattering with mitoplasts (*Mp*) and whole mitochondria (*Mc*). A remarkable increase in scattered light (shrinkage) is observed when the specimens are subjected rapidly to a hypertonic osmotic gradient of 140 mosM. No change in scattered light is observed when the samples are mixed with iso-osmotic buffer (absence of osmotic gradient). (B) The rate constant (K_i) of the specimens examined is high (black histograms). Significant reductions in the K_i value are observed in all samples after treatment with 300 μM $HgCl_2$ (dotted histograms). Proving the absence of artefacts, the inhibition in all samples is reversed by 15 min treatment with 10 mM of the reducing agent β-mercaptoethanol (striped histograms). Data are mean values±S.E. from five independent preparations for each specimen. Asterisk (*), $p<0.0001$.

level of its membrane subcompartments. High water permeability was measured with the OMM and IMM vesicles, whose K_i values were 29.70±4.2 and 30.33±4.5 s^{-1}, respectively (Fig. 5A, B; *black histograms*). These values were much higher than the rate constant of 2.67±1.8 s^{-1} related to the simple diffusion of water across liposome models of the rat liver IMM lipid bilayer (Fig. 5A; *LS*). Because the K_i is not very informative regarding the extent and nature of membrane water permeability, we decided to calculate the coefficient of the osmotic water permeability, P_f, by applying the van Heeswijk and van Os equation [17]. The P_f of the liver IMM vesicles was eight times higher than that of the related protein-free IMM liposomes (451±52 vs 57±6 μm s^{-1}, respectively; Fig. 5C) while it was not significantly different from the P_f values measured with the brain and testis IMM vesicles (437±61 and 422±49 μm s^{-1}, respectively). Calculation of the liver OMM P_f was also attempted (411±48 μm s^{-1}), despite the presence of VDAC, a channel freely permeable to molecules up to 1.5 kDa with an exceedingly large pore (20 Å in the outer membrane of *Neurospora crassa* mitochondria [21] which could mediate a mass movement of fluid i.e. water and solutes across the same pore, simultaneously).

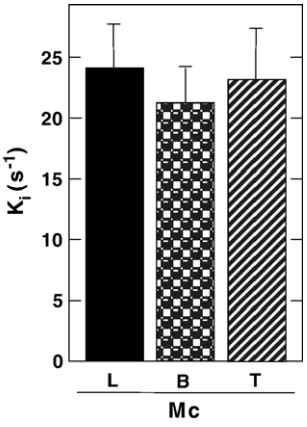

Fig. 4. Stopped flow light scattering analyses of brain and testis mitochondria. The rate constants of the osmotic water efflux out of both testis (*T*) and brain (*B*) mitochondria are remarkably high and not significantly different from that measured for liver (*L*) mitochondria. *Mc*, mitochondria.

Another series of light scattering experiments was performed using $HgCl_2$, a mercurial compound known to block water permeability by acting on the sulfhydryl group of cysteines in the vicinity of proteinaceous aqueous pores [22]. The extent of K_i inhibition by the Hg^{++} ion for mitochondria and mitoplasts was −24.8±4.5% and −47.2±9.4%, respectively (Fig. 3B), whereas the percentage of rate constant reduction for the OMM and IMM vesicles was −43.5±11.7% and −52.1±8.9%, respectively (Fig. 5B). Similar extents of Hg^{++} inhibition of water transport were obtained when the hypertonic osmotic gradient was created by sucrose (Fig. 5D), an osmolyte of higher molecular mass than mannitol and one that is impermeable across any known aquaporin. Indicating no changes of the kinetics of osmotic equilibration resulting from alterations in vesicle surface-to-volume ratio or aggregation induced by Hg^{++} treatment, no significant changes to vesicle diameter were observed with the specimens exposed to Hg^{++} (data not shown). All together, these results confirm the existence of Hg^{++}-sensitive pathways of water movement. The above inhibitions were reversed after incubation with β-mercaptoethanol (Fig. 5B, D).

To examine further the molecular mechanism and pathway (s) of water transport across IMM, we decided to determine the Arrhenius activation energy (E_a) of the osmotic water permeability of the whole intact liver mitochondria (6000×g fraction) from temperature dependence data. Some increase in the rate of osmotic water transport was observed when the mitochondria

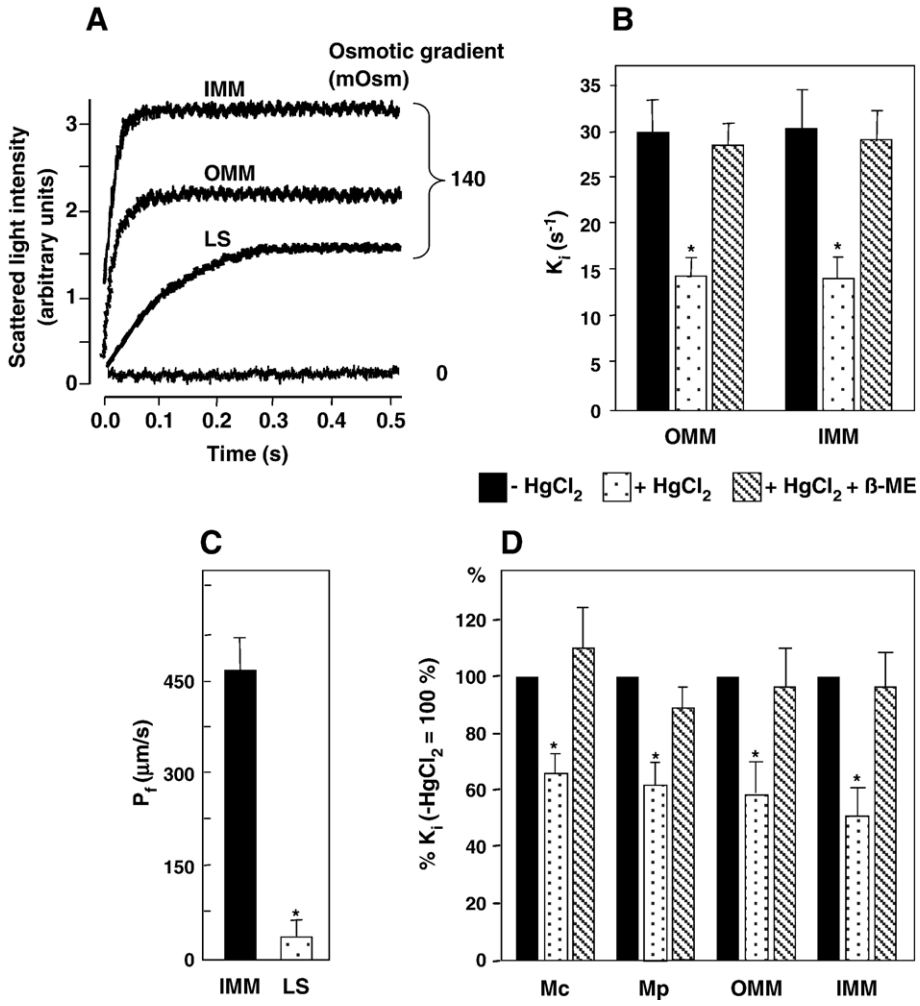

Fig. 5. Biophysical analysis of water transport across liver OMM and IMM vesicles and model liposomes of the IMM lipid bilayer. (A) representative experiments of stopped flow light scattering with outer (*OMM*) and inner (*IMM*) membrane vesicles and liposomes made up of the lipid composing the liver IMM bilayer (*LS*). A remarkable increase in scattered light (shrinkage) is observed when the OMM and IMM vesicles are subjected rapidly to a hypertonic osmotic gradient of 140 mosM. A slight increase in scattered light is observed with liposomes. No change in scattered light is observed when the samples are mixed with iso-osmotic buffer. (B) The rate constant (K_i) of the OMM and IMM vesicles is strikingly elevated. Significant reductions in the K_i value are observed in all samples after treatment with 300 µM $HgCl_2$. The inhibition in both samples is reversed by 15 min treatment with 10 mM of β-mercaptoethanol. (C) Osmotic water permeabilities (P_f) of the IMM vesicles and liposomes (LS). (D) Percentage of Hg^{++}-inhibition and related reversal by βmercaptoethanol of the rate constants measured after exposure to a hypertonic osmotic gradient of 140 mosM made by sucrose. Data are mean values±S.E. from five independent preparations for each specimen. Asterisk (*), $p<0.0001$.

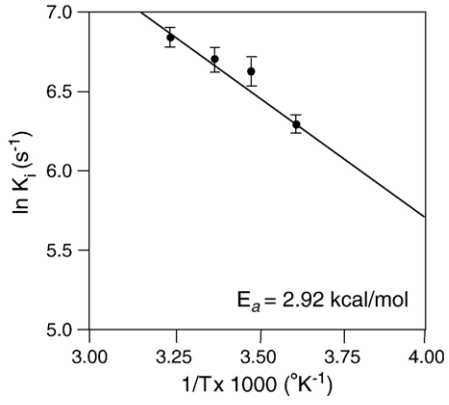

Fig. 6. Arrhenius activation energy (E_a) of osmotic water transport in liver mitochondria. The Arrhenius plotting is obtained with the rate constant values (hyperosmotic gradient of 140 mosM) of mitochondria measured at 5, 15, 25 and 37 °C resulting in an E_a of 2.92 kcal/mole.

were subjected to the same osmotic gradient (140 mosM) at increasing temperatures. Arrhenius plotting of the rate constant values at 5, 15, 25 and 37 °C resulted in an E_a of 2.92 kcal/mole (Fig. 6), a low value and, therefore, biophysically consistent with water permeation through aqueous pores [17].

4. Discussion

The movement of water between the mitochondrial matrix and the cytoplasm underlies the plasticity of the mitochondrial shape and is central in the homeostatic control of mitochondrial volume [23]. This study employed stopped flow light scattering to characterize biophysically the water permeabilities of rat mitochondria, mitoplasts and outer and inner mitochondrial membranes. Experiments with compounds known to block the water permeability of proteinaceous aqueous pores were also carried out. All together, the results indicate that (i) the whole

mitochondrion is highly permeable to water, (ii) the water permeabilities of the OMM and IMM are of comparable extent and (iii) in spite of their high surface-to-volume ratio, a feature that can justify millisecond osmotic equilibration, mitochondria possess facilitated pathways for water diffusion other than the AQP8 water channels.

Two important biophysical parameters in characterizing the water permeability of mitochondria and their subcompartments are the rate constant of shrinkage/swelling (K_i) and the coefficient of osmotic permeability (P_f). However, while the P_f is very informative on the channel-mediated water permeability, the K_i provides limited information as it depends on the P_f and the surface-to-volume ratio of the specimen analyzed. In this work, the K_i values were used to evaluate the inhibition by the Hg^{++} ion and calculate the Arrhenius activation energy (E_a). The P_f calculation was not problematic with the OMM and IMM vesicles, while with mitochondria and mitoplasts it was hampered by biophysical (presence of two membranes in series in mitochondria) and morphological (rod-shaped structures of heterogeneous size) constraints. However, a rough estimation of the mitochondrial P_f could be speculatively attempted by applying the van Heeswijk and van Os equation [17] and employing the mean length, external surface area and volume value of mitochondria reported by Safiulina and coworkers in a recent paper using confocal microscopy [1]. Such estimation leads to a mitochondrial P_f of $\approx$400 μm s^{-1}, a value of extraordinarily high extent. Because the single channel water permeability (P_f) of a standard mammalian aquaporin such as AQP1 was reported to correspond to $\approx 6\times 10$–14 cm^3 s^{-1} [24,25], it can be also estimated that mitochondria have a striking density of over 6000 aquaporin-equivalent water channels per μm^2 of external membrane surface area. However, while underlining the high water conductance of mitochondria this estimation does not mean that the intrinsic membrane water permeability of mitochondria is due to aquaporins. The functional significance of aquaporins such as AQP8 and AQP9 in mitochondria has been a matter of debate ever since the overall water or glycerol permeabilities of mitochondria isolated from AQP8 or AQP9 knockout were reported not to differ from those of mitochondria from wildtype mice [14]. This is consistent with our observation that the overall water permeability of brain mitochondria that lack AQP8 water channels corresponds to that of liver and testis mitochondria that, by contrast, have the AQP in question in their IMMs [10]. Because AQP8 shows considerable immunoreactivity in subpopulations of liver mitochondria characterized by their large diameter [10], it may be reasonable to think that mitochondrial AQP8 might have physiological relevance in heavy mitochondria. Rat liver AQP8 has been suggested to play a role in the metabolism of amino acids by mediating the mitochondrial uptake of NH4+ to supply the urea cycle [26]. Such hypothesis is not supported by a recent work by Yang and coworkers who used AQP8 null knockout mice to provide evidence against physiologically significant AQP8 facilitated ammonia transport [27]. Clues in assessing the functional meaning of mitochondrial AQP8 may come from our preliminary observation that AQP8 is absent in the mitochondrial compartments of immortalized mouse hepatocytes (no apoptosis) and rat spermatozoa (no β-oxidation of fatty acids). Overall, an open question relates to the meaning of the presence of aquaporin water channels in organelles with high surface-to-volume ratio such as mitochondria [9,10] and secretory vesicles [28] having osmotic equilibration times in the order of tens of milliseconds. The question is currently being fiercely debated [14,29,30] and is a matter for further investigation.

The fact that the K_i of the mitoplasts and IMM vesicles was only partially reduced by the Hg^{++} ion (−47% and −52%, respectively), an aquaporin blocker, confirms our previous study [10] and corroborates the existence of additional pathways other than AQP8 mediating the movement of water across the IMM. Further support from the hypothesis of a facilitated pathway comes from (i) the low activation energy associated to the osmotic water transport, (ii) the fact that no significant alterations in size were observed after exposing the mitochondria or the vesicles to $HgCl_2$ and (iii) the experiments with the liposomes indicating minor importance for water transport through the lipid bilayer. A potentially important candidate in explaining the high water permeability featured by mitochondria is the permeability transition pore (PTP), a polyprotein complex formed at contact points between the inner and the outer mitochondrial membranes known to be directly involved in mitochondrial volume homeostasis [31]. The molecular conductance of PTP is dynamically affected by many factors [15], a critical aspect in assessing the mitochondrial molecular conductances. Work is in progress in our laboratory to evaluate biophysically the importance of PTP in the mitochondrial water permeability.

The fact that the water permeability found for OMM vesicles was high but of similar extent compared to that obtained with the IMM vesicles was surprising, since the outer membrane is commonly believed to represent a relatively minor barrier (i.e. compared to the IMM) for molecules moving between the mitochondrion and its surrounding cytoplasm [7]. This unexpected result could be due to the fact that in the preparations submitted to light scattering the VDAC, the main route for molecules moving across the OMM [7,32], was only partially open. Complete (or almost complete) VDAC closure is known to occur in many ways (including colloidal osmotic pressure created by inaccessible polymers [33] and involve a reduction in the overall conductance of the channel (generally a 50–60% reduction) [34]. An answer to the question may derive from future studies where the water permeabilities featured by outer membranes with VDAC in its open and closed states, respectively, will be specifically addressed.

In conclusion, while biophysically characterizing water movement across the mitochondrion and its subcompartments, this study provides important insights into the knowledge of the homeostatic mechanisms underlying mitochondrial plasticity. The existence of major membrane pathways of water movement other than AQP8 is also suggested. Important insights should be provided from studies aimed at investigating the possible role of

VDAC and PTP, both in their open state, in mitochondrial water permeability.

Acknowledgments

This work is dedicated to the memory of Barbara Baldacci, unforgettable undergraduate student in our laboratory. We are grateful to the financial support provided by PRIN (Programma di Ricerca Scientifica di Interesse Rilevante; G.C.), LAG (Laboratorio del Gene; G.C. and M.S.) and CEGBA (Centro di Eccellenza di Genomica in campo Biomedico ed Agrario; G.C. and M.S.), to Profs. Silvia Micelli and Enrico Gallucci for their contribution to the biophysical studies and their valuable suggestions, to Dr. Marco Colombini for his valuable suggestions, to Drs. Elena Fanelli and Marianna Spagnulo for their helpful contribution to the experiments.

References

[1] D. Safiulina, V. Veksler, A. Zharkovsky, A. Kaasik, Loss of mitochondrial membrane potential is associated with increase in mitochondrial volume: physiological role in neurones, J. Cell. Physiol. 206 (2006) 347–353.
[2] S. Desagher, J.C. Martinou, Mitochondria as the central control point of apoptosis, Trends Cell Biol. 10 (2000) 369–377.
[3] W.K. Lee, F. Thevenod, A role for mitochondrial aquaporins in cellular life and death decisions? Am. J. Physiol. Cell Physiol. 291 (2006) C195–C202.
[4] K.D. Garlid, P. Paucek, Mitochondrial potassium transport: the $K^{(+)}$ cycle, Biochim. Biophys. Acta 1606 (2003) 23–41.
[5] K.D. Garlid, Cation transport in mitochondria—The potassium cycle, Biochim. Biophys. Acta 1275 (1996) 123–126.
[6] T. Kristian, J. Gertsch, E.T. Bates, B.K. Siesjö, Characteristics of the calcium-triggered mitochondrial permeability transition in nonsynaptic brain mitochondria: effect of cyclosporin A and ubiquinone O, J. Neurochem. 74 (2000) 1999–2009.
[7] M. Colombini, VDAC: the channel at the interface between mitochondria and the cytosol, Mol. Cell. Biochem. 256–257 (2004) 107–115.
[8] F. Palmieri, The mitochondrial transporter family (SLC25): physiological and pathological implications, Pflügers Arch.-Eur. J. Physiol. 447 (2004) 689–709.
[9] D. Ferri, A. Mazzone, G.E. Liquori, G. Cassano, M. Svelto, G. Calamita, Ontogeny, distribution, and possible functional implications of an unusual aquaporin, AQP8, in mouse liver, Hepatology 38 (2003) 947–957.
[10] G. Calamita, D. Ferri, P. Gena, G.E. Liquori, A. Cavalier, D. Thomas, M. Svelto, The inner mitochondrial membrane has aquaporin-8 water channels and is highly permeable to water, J. Biol. Chem. 280 (2005) 17149–17153.
[11] W.K. Lee, U. Bork, F. Gholamrezaei, F. Thevenod, Cd(2+)-induced cytochrome c release in apoptotic proximal tubule cells: role of mitochondrial permeability transition pore and Ca(2+) uniporter, Am. J. Physiol.: Renal Physiol. 288 (2005) F27–F39.
[12] M. Amiry-Moghaddam, H. Lindland, S. Zelenin, B.A. Roberg, B.B. Gundersen, P. Petersen, E. Rinvik, I.A. Torgner, O.P. Ottersen, Brain mitochondria contain aquaporin water channels: evidence for the expression of a short AQP9 isoform in the inner mitochondrial membrane, FASEB J. 19 (2005) 1459–1467.
[13] K. Ishibashi, M. Kuwahara, Y. Kageyama, A. Tohsaka, F. Marumo, S. Sasaki, Cloning and functional expression of a second new aquaporin abundantly expressed in testis, Biochem. Biophys. Res. Commun. 237 (1997) 714–718.
[14] B. Yang, D Zhao, A.S. Verkman, Evidence against functionally significant aquaporin expression in mitochondria, J. Biol. Chem. 281 (2006) 16202–16206.
[15] M. Crompton, The mitochondrial permeability transition pore and its role in cell death, Biochem. J. 341 (Pt 2) (1999) 233–249.
[16] G. Daum, Lipids of mitochondria, Biochim. Biophys. Acta 822 (1985) 1–42.
[17] M.P. van Heeswijk, C.H. van Os, Osmotic water permeabilities of brush border and basolateral membrane vesicles from rat renal cortex and small intestine, J. Membr. Biol. 92 (1986) 183–193.
[18] J. Bereiter-Hahn, Behavior of mitochondria in the living cell, Int. Rev. Cytol. 122 (1990) 1–63.
[19] Y. Koyama, T. Yamamoto, D. Kondo, H. Funaki, E. Yaoita, K. Kawasaki, N. Sato, K. Hatakeyama, I. Kihara, Molecular cloning of a new aquaporin from rat pancreas and liver, J. Biol. Chem. 272 (1997) 30329–30333.
[20] T. Ma, B. Yang, A.S. Verkman, Cloning of a novel water and urea-permeable aquaporin from mouse expressed strongly in colon, placenta, liver, and heart, Biochem. Biophys. Res. Commun. 240 (1997) 324–328.
[21] C.A. Mannella, M. Colombini, J. Frank, Structural and functional evidence for multiple channel complexes in the outer membrane of *Neurospora crassa* mitochondria, Proc. Natl. Acad. Sci. U. S. A. 80 (1983) 2243–2247.
[22] G.M. Preston, J.S. Jung, W.B. Guggino, P. Agre, The mercury-sensitive residue at cysteine 189 in the CHIP28 water channel, J. Biol. Chem. 268 (1993) 17–20.
[23] A.D. Beavis, R.D. Brannan, K.D. Garlid, Swelling and contraction of the mitochondrial matrix. I. A structural interpretation of the relationship between light scattering and matrix volume, J. Biol. Chem. 260 (1985) 13424–13433.
[24] A.N. van Hoek, A.S. Verkman, Functional reconstitution of the isolated erythrocyte water channel CHIP28, J. Biol. Chem. 267 (1992) 18267–18269.
[25] B. Yang, A.S. Verkman, Water and glycerol permeabilities of aquaporins 1–5 and MIP determined quantitatively by expression of epitope-tagged constructs in *Xenopus* oocytes, J. Biol. Chem. 272 (1997) 16140–16146.
[26] L.M. Holm, T.P. Jahn, A.L. Moller, J.K. Schjoerring, D. Ferri, D.A. Klaerke, T. Zeuthen, NH3 and NH4+ permeability in aquaporin-expressing *Xenopus* oocytes, Pflugers Arch. 450 (2005) 415–428.
[27] B. Yang, D. Zhao, E. Solenov, A.S. Verkman, Evidence from knockout mice against physiologically significant aquaporin-8 facilitated ammonia transport, Am. J. Physiol. Cell Physiol. (in press) (doi:10.1152/ajpcell.00057.2006).
[28] S.J. Cho, B.P. Jena, Secretory vesicle swelling by atomic force microscopy, Methods Mol. Biol. 319 (2006) 317–330.
[29] A.S. Verkman, More than just water channels: unexpected cellular roles of aquaporins, J. Cell Sci. 118 (2005) 3225–3232.
[30] A. Hill, Salt-water coupling in leaky epithelia, J. Membr. Biol. 56 (1980) 177–182.
[31] M.G. Vander Heiden, N.S. Chandel, E.K. Williamson, P.T. Schumacker, C. B. Thompson, Bcl-xL regulates the membrane potential and volume homeostasis of mitochondria, Cell 91 (1997) 627–637.
[32] A.C. Lee, X. Xu, E. Blachly-Dyson, M. Forte, M. Colombini, The role of yeast VDAC genes on the permeability of the mitochondrial outer membrane, J. Membr. Biol. 161 (1998) 173–181.
[33] J. Zimmerberg, V.A. Parsegian, Polymer inaccessible volume changes during opening and closing of a voltage-dependent ionic channel, Nature 323 (1986) 36–39.
[34] M. Colombini, Voltage gating in VDAC: toward a molecular mechanism, in: C. Miller (Ed.), Ion Channel Reconstitution (Section 4) Chapter 10, Plenum Press, New York, 1986.